

# Organic Carbon/Water and Dissolved Organic Carbon/Water Partitioning of Cyclic Volatile Methylsiloxanes: Measurements and Polyparameter Linear Free Energy Relationships

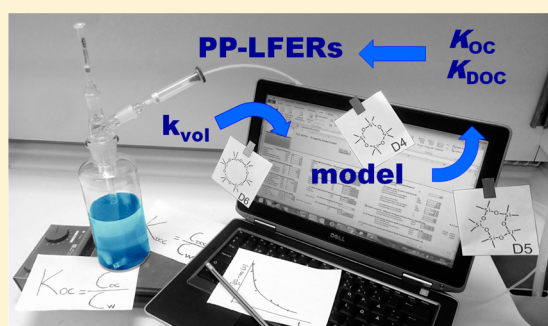
Dimitri Panagopoulos,<sup>\*,†</sup> Annika Jahnke,<sup>†,‡</sup> Amelie Kierkegaard,<sup>†</sup> and Matthew MacLeod<sup>†</sup>

<sup>†</sup>Department of Environmental Science and Analytical Chemistry, ACES, Stockholm University, Svante Arrhenius väg 8, SE-114 18 Stockholm, Sweden

<sup>‡</sup>Department of Cell Toxicology, Helmholtz Centre for Environmental Research, UFZ, Permoserstraße 15, DE-04318 Leipzig, Germany

## S Supporting Information

**ABSTRACT:** The sorption of cyclic volatile methyl siloxanes (cVMS) to organic matter has a strong influence on their fate in the aquatic environment. We report new measurements of the partition ratios between freshwater sediment organic carbon and water ( $K_{OC}$ ) and between Aldrich humic acid dissolved organic carbon and water ( $K_{DOC}$ ) for three cVMS, and for three polychlorinated biphenyls (PCBs) that were used as reference chemicals. Our measurements were made using a purge-and-trap method that employs benchmark chemicals to calibrate mass transfer at the air/water interface in a fugacity-based multimedia model. The measured  $\log K_{OC}$  of octamethylcyclotetrasiloxane ( $D_4$ ), decamethylcyclopentasiloxane ( $D_5$ ), and dodecamethylcyclohexasiloxane ( $D_6$ ) were 5.06, 6.12, and 7.07, and  $\log K_{DOC}$  were 5.05, 6.13, and 6.79. To our knowledge, our measurements for  $K_{OC}$  of  $D_6$  and  $K_{DOC}$  of  $D_4$  and  $D_6$  are the first reported. Polyparameter linear free energy relationships (PP-LFERs) derived from training sets of empirical data that did not include cVMS generally did not predict our measured partition ratios of cVMS accurately (root-mean-squared-error (RMSE) for  $\log K_{OC}$  0.76 and for  $\log K_{DOC}$  0.73). We constructed new PP-LFERs that accurately describe partition ratios for the cVMS as well as for other chemicals by including our new measurements in the existing training sets ( $\log K_{OC}$  RMSE<sub>cVMS</sub>: 0.09,  $\log K_{DOC}$  RMSE<sub>cVMS</sub>: 0.12). The PP-LFERs we have developed here should be further evaluated and perhaps recalibrated when experimental data for other siloxanes become available.



## INTRODUCTION

Cyclic volatile methylsiloxanes (cVMS) have recently attracted the attention of environmental chemists and regulators because of their high production and release rates,<sup>1–3</sup> their presence in the aquatic environment<sup>4</sup> and their bioaccumulation potential.<sup>5</sup> cVMS are mainly used as monomers in the production of polymeric silicones and as carriers in personal care products.<sup>1–3</sup> On a smaller scale, cVMS are also used as lubricants and solvents in a variety of commercial applications.<sup>1–3</sup> The most widely used cVMS are octamethylcyclotetrasiloxane ( $D_4$ ), decamethylcyclopentasiloxane ( $D_5$ ), and dodecamethylcyclohexasiloxane ( $D_6$ ).<sup>1–3</sup>

cVMS are volatile ( $\log$  air/water partition ratio  $K_{AW}$  of  $D_5$ : 3.13<sup>6</sup>) and highly hydrophobic ( $\log$  octanol/water partition ratio  $K_{OW}$  of  $D_5$ : 8.07<sup>6</sup>). According to risk assessments conducted by the British Environment Agency,<sup>1–3</sup> the largest emissions of cVMS are from personal care products and occur to air. Due to their volatility cVMS that are emitted to air remain in the atmosphere until they are removed by reacting with hydroxyl radicals.<sup>7–9</sup> A smaller fraction of cVMS is released to surface waters via sewage treatment plants. Due to

their hydrophobicity, cVMS are likely to be sorbed to suspended particles in sewage treatment plant effluent and deposit onto surface sediment. cVMS undergo hydrolysis in water, however, the residence time of cVMS in rivers and lakes depends strongly on the amount and quality of organic carbon present in the dissolved phase, in the suspended particles and in the sediment.<sup>10,11</sup> Therefore, the partition ratios of cVMS between organic carbon and water ( $K_{OC}$ ) and dissolved organic carbon and water ( $K_{DOC}$ ) are key parameters that are required to understand the fate of cVMS in the aquatic environment.

Measurements of  $K_{OC}$  and  $K_{DOC}$  for organic chemicals have been used to calibrate empirical models. Single-parameter linear free energy relationships (SP-LFERs), such as the Seth,<sup>12</sup> the Karickhoff,<sup>13,14</sup> and the Burkhard<sup>15</sup> regression equations, relate the  $K_{OC}$  or  $K_{DOC}$  of a chemical to the chemical's  $K_{OW}$ . Using a  $\log K_{OW}$  of 8.07 for  $D_5$ ,<sup>6</sup> the Seth regression<sup>12</sup> estimates a  $\log$

Received: May 20, 2015

Revised: August 28, 2015

Accepted: September 15, 2015

Published: September 15, 2015

$K_{OC}$  of 7.57. Previous experimental studies have reported considerably lower  $\log K_{OC}$  values that range from 4.98 to 6.33 for  $D_5$ .<sup>10,11,16</sup> These values for  $D_5$  are all more than 1 order of magnitude lower than the estimate from the Seth regression. Existing SP-LFERs fail to provide good estimates for cVMS because SP-LFERs implicitly assume that controlling interactions are identical for all chemicals. SP-LFERs are chemical class-specific, and thus they should not be extrapolated across chemical classes.<sup>17</sup> Existing SP-LFERs have been constructed using measured data for chlorinated hydrocarbon-based chemicals and nonhalogenated hydrocarbon-based chemicals but not organosilicon chemicals,<sup>12–15</sup> and to our knowledge empirical data for  $K_{DOC}$  of  $D_4$  and  $D_6$  and  $K_{OC}$  of  $D_6$  have not yet been reported.

In contrast to SP-LFERs, polyparameter linear free energy relationships (PP-LFERs) can be applied across chemical classes. PP-LFERs are composed of multiplicative terms that describe molecular interactions controlling the partitioning of an organic chemical between two phases.<sup>18</sup> Three examples of PP-LFER equations are:<sup>19–21</sup>

$$\log K = sS + aA + bB + eE + vV + c \quad (\text{EV model}) \quad (1)$$

$$\log K = sS + aA + bB + eE + lL + c \quad (\text{EL model}) \quad (2)$$

$$\log K = sS + aA + bB + vV + lL + c \quad (\text{VL model}) \quad (3)$$

Each multiplicative term in a PP-LFER consists of a solute descriptor that is a property of the chemical, and a solvent descriptor that is a property of the two solvent phases in the partition ratio. The capital letters are the solute descriptors and describe the following properties; *S*, dipole–dipole interactions; *A*, hydrogen bonding (H-donor); *B*, hydrogen bonding (H-acceptor); *E*, dispersive forces and dipole–induced dipole interactions; *V*, McGowan's characteristic molecular volume; *L*, partition ratio between air and hexadecane. The small letters are the solvent descriptors and describe the following properties; *s*, difference in the tendencies of the two solvents for dipole–dipole interactions; *a*, difference in the tendencies of the two solvents to accept hydrogen bonds from the solute; *b*, difference in the tendencies of the two solvents to donate hydrogen bonds to the solute; *e*, difference in the tendencies of the two solvents for dispersive forces and dipole–induced dipole interactions with the solute; *v*, difference in the cohesive energy of the two solvents; *l*, difference in the tendencies of the two solvents to form London dispersion forces and dipole–induced dipole interactions; and *c* is a constant.

Abraham et al. proposed the EV model (eq 1)<sup>19</sup> for partitioning between two condensed phases and the EL model (eq 2)<sup>20</sup> for partitioning between a condensed phase and the gas phase. The VL model (eq 3) was proposed by Goss<sup>21</sup> for both condensed–condensed and gaseous–condensed partitioning. eqs 1 and 2 were applied successfully to describe the partition ratios of chlorinated hydrocarbons and nonhalogenated hydrocarbons but do not perform well for organosilicon and polyfluorinated compounds.<sup>22</sup> This observation led Endo and Goss<sup>22</sup> to recommend eq 3. However, they noted that the solvent descriptors of PP-LFERs based on eq 3 need to be refined since these chemical classes were not included in the training sets.<sup>22</sup>

The first goal of this study was to measure the partitioning of cVMS between organic carbon and water and provide the first

empirical data for  $K_{DOC}$  of  $D_4$  and  $K_{OC}$  and  $K_{DOC}$  of  $D_6$ . The organic carbon in the  $K_{OC}$  measurements came from freshwater sediment and the organic carbon in the  $K_{DOC}$  measurements is Aldrich humic acids. Due to the extreme difficulty of accurately determining concentrations of cVMS in water with current methods, we measured  $K_{OC}$  and  $K_{DOC}$  indirectly in a purge-and-trap system that allows for mass balance analysis. The system also mimics emissions of chemicals to water in association with organic carbon. Simultaneously and in the same system, we measured the partition ratios of three PCBs, which are chemicals with well-defined  $K_{OC}$  that were used as reference chemicals to provide additional confidence to our method. We compared our experimental results to other measurements in the literature for PCBs,  $D_4$  and  $D_5$ , to the predictions of PP-LFERs derived from existing data sets. Our second goal was to combine our new measurements with existing data to construct PP-LFERs of the form of eq 3 that describe  $\log K_{OC}$  and  $\log K_{DOC}$  for diverse sets of compounds that include cVMS.

## METHODS AND MATERIALS

**Summary of the Partitioning Experiments.** The experimental design was inspired by the work of Whelan et al.<sup>10,11</sup> who conducted experiments using open beakers, where  $K_{OC}$  was determined indirectly via the chemicals' volatilization rate. Instead of open beakers,<sup>10,11</sup> we used a closed system (Figure 1) that allows for calculations of the chemicals' mass

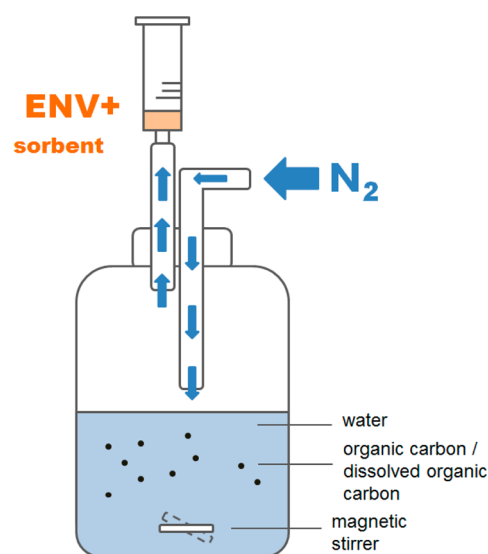


**Figure 1.** Schematic illustration of the purge-and-trap system. Water volume = 300 mL, nitrogen flow = 25 mL/min, sampling time points = 2, 4, 8, 12, 24, 48, and 72 h.

balance. Two benchmark chemicals, 1,4-dichlorobenzene (DCB) and  $\alpha$ -hexachlorocyclohexane ( $\alpha$ -HCH), were used to calibrate the mass transfer coefficients at the air–water interface in our fugacity model of the purge-and-trap system. We included three PCBs in our experiments as reference chemicals with well-characterized partitioning properties. In the  $K_{OC}$  experiments, a mixture of cVMS, PCBs, 1,4-DCB, and  $\alpha$ -HCH was spiked onto field sediment collected from a Swedish freshwater lake (organic carbon content: 6.4%) representing bulk organic carbon. The spiked sediment was added to a continuously stirred volume of water in the purge-and-trap system. The procedure is described in detail in the Supporting Information, SI, Text S1. In the DOC experiments, the

chemical mixture was spiked under the water surface after Aldrich humic acid had been dissolved in the water. The headspace of the system was continuously purged with a gentle stream of nitrogen (25 mL/min), which carried chemicals in the gas phase to a solid-phase extraction (SPE) column packed with 25 mg of ENV+ resin.<sup>23</sup> After 2, 4, 8, 12, 24, 48, and 72 h, the ENV+ columns were exchanged and the amount of the chemicals collected was measured after eluting the columns with 1 mL dichloromethane into GC vials. Additionally, at the end of the experiment, the bulk water containing sediment or Aldrich humic acid was analyzed to assess the mass balance and to confirm that no substantial losses of the chemicals due to degradation or breakthrough had occurred. The methods are presented in detail in SI, Text S2. We determined partition ratios between water and organic carbon by fitting the measured amounts of volatilized chemicals using a multimedia model with mass transfer coefficients at the air–water interface calibrated using our observations of DCB and  $\alpha$ -HCH (see Modeling section).

**Materials.** D<sub>4</sub>, D<sub>5</sub>, 1,4-DCB,  $\alpha$ -HCH and Aldrin standards, methanol, potassium hydroxide (KOH) as well as Aldrich humic acid were purchased from Sigma-Aldrich Sweden AB, Stockholm, Sweden. Although, Aldrich humic acid has been reported to have different sorption properties than dissolved organic carbon from the natural environment,<sup>24</sup> we selected it for our study for consistency with measurements by Whelan et al.<sup>10</sup> for D<sub>5</sub> and because there is an existing PP-LFER equation for  $K_{\text{DOC}}$  using Aldrich humic acid.<sup>25</sup> D<sub>6</sub> was purchased from Fluorochem, Derbyshire, U.K. <sup>13</sup>C<sub>4</sub>-D<sub>4</sub>, <sup>13</sup>C<sub>5</sub>-D<sub>5</sub>, and <sup>13</sup>C<sub>6</sub>-D<sub>6</sub> were purchased from Moravsek Biochemicals Inc., Brea, California, U.S.A. PCB 28, PCB 52, PCB 53, PCB 153, <sup>13</sup>C<sub>12</sub>-PCB 28, <sup>13</sup>C<sub>12</sub>-PCB 52, and <sup>13</sup>C<sub>12</sub>-PCB 153 were purchased from Larodan, Solna, Sweden. The Isolute ENV+ resin (hydroxylated polystyrene-divinylbenzene copolymer) was purchased from Biotage AB (Uppsala, Sweden). Dichloromethane and *n*-hexane were purchased from Merck (Darmstadt, Germany). Concentrated sulfuric acid (98%) was purchased from BDH AnalAR (Poole, England).

Sediment used as a source of bulk organic carbon including particulate and dissolved organic carbon was collected from Lake Ången, Sweden and is described in the study of Jahnke et al.<sup>26</sup> Water was filtered and deionized using a Milli-Q system (Merck Millipore, Solna, Sweden).

**Quality Assurance/Quality Control.** Due to their presence in personal care products, the analysis of cVMS is prone to contamination issues. Although we spiked chemicals at levels that greatly exceed background levels, we took precautions to control the levels of background contamination. Exposure to any type of rubber/silicon septa was avoided by covering the openings of the tubes containing the standards with aluminum foil before putting their caps on. Blank samples were run along with each extraction batch and were analyzed together with the samples. The standards were renewed once per month. Method detection limits (MLD) and method quantification limits (MQL) were calculated from the blanks that were run along with our samples. The MDL was defined as the average concentration of each analyte in the blanks plus three times the standard deviation, and the MQL was defined as the average concentration of each analyte plus ten times the standard deviation. The MDL and MQL for each compound are presented in Table S3.

## MODELING

We fit the measured volatilization rate of chemicals from the system during each experiment with a first order kinetic model eq 4 that accounts for the formation of a nonavailable fraction and degradation of chemical in the system:

$$I(t) = (100 - b(t))e^{-kt} + b(t) \quad (4)$$

where  $I(t)$  is the percentage of spiked compound remaining in the system at time  $t$ ,  $k$  is the rate constant for volatilization of the compound from the system, and  $b(t)$  is the percentage of chemical that is not available for volatilization because it has been degraded in the bulk water phase, and/or because of the formation of a nonavailable fraction that cannot enter the dissolved phase in water. Other possible loss mechanisms include adsorption of the chemicals to the glass surfaces, leakage when changing cartridges and breakthrough.

Formation of the nonavailable fraction was described as a first-order process assuming that 100% of the chemical is available for volatilization at time zero eq 5:

$$b(t) = B(1 - e^{-k_b t}) \quad (5)$$

where  $b(t)$  is the amount of the nonavailable fraction at time  $t$ ,  $B$  is the maximum amount of the nonavailable fraction in the system, and  $k_b$  is the formation rate constant for the nonavailable fraction. Measurements from each experiment were fit by least-squares minimization by optimizing values of  $k$ ,  $B$ , and  $k_b$  for eqs 4 and 5 using the Solver function in Microsoft Excel.<sup>27</sup>

We used a fugacity-based multimedia model parametrized to describe the experimental system to calculate the organic carbon–water partition ratio from  $k$  determined from fitting our experimental data (Text S3). The model assumes equilibrium partitioning between organic carbon and water, and nonequilibrium conditions between air and water. The measured volatilization rates of 1,4-DCB and  $\alpha$ -HCH were used to calibrate the mass transfer coefficients (MTCs) for air–side mass transfer at the air–water interface ( $\text{MTC}_a$ ) and water–side mass transfer at the air–water interface ( $\text{MTC}_w$ ) respectively. A detailed description of the model is given in Text S3.

We adjusted the partition ratio between organic carbon and water in the calibrated fugacity model to fit our experimentally determined rate constants,  $k$  for transfer of chemical from bulk water that is composed of pure water and the sorbent to the ENV+ trap. The fraction of chemical in the dissolved phase in water,  $\phi_{\text{dissolved}}$  is:

$$\phi_{\text{dissolved}} = kt_{w \rightarrow \text{ENV}+} \quad (6)$$

where,  $t_{w \rightarrow \text{ENV}+}$  is the characteristic time for the chemical to move from the dissolved phase in water to the ENV+ trap, as determined by the calibrated model.

The  $K_{\text{OC}}$  or  $K_{\text{DOC}}$  that were adjusted in the model are related to  $\phi_{\text{dissolved}}$  as follows:

$$K_{\text{OC}} \text{ or } K_{\text{DOC}} = \left( \frac{1}{\phi_{\text{dissolved}}} - 1 \right) \frac{V_w}{V_s} \quad (7)$$

Where,  $V_w$  is the volume of water, and  $V_s$  is the volume of OC or DOC in the system.

**PP-LFERs.** We constructed new PP-LFERs from existing data sets based on the approach suggested by Goss.<sup>21</sup> Two separate data sets that were compiled by Nguyen et al.<sup>28</sup> and



Bronner et al.<sup>29</sup> were used to construct log  $K_{OC}$  PP-LFERs. The data set for the log  $K_{DOC}$  PP-LFER for Aldrich humic acid was compiled by Neale et al.<sup>25</sup> After evaluating the performance of these PP-LFERs against our new measurements for PCBs and cVMS, we constructed new PP-LFER models that include our measurements in the training sets. The substance PP-LFER descriptors that were used for the newly constructed PP-LFERs are presented in Table S7.

**Data Analysis.** Statistical analysis was conducted in Microsoft Excel 2010. Differences were considered as significant when  $p < 0.05$ . Root-mean-squared-error (RMSE) was used to evaluate the performance of PP-LFER models for various subsets of the experimental data.

## RESULTS

**Mass Balance Control.** The average total recoveries from ENV+ traps and total extraction of water at the end of experiments ( $n = 4$ ) ranged from 70 to 90% for cVMS and from 78 to 108% for PCBs and benchmarks in the  $K_{OC}$  experiments and 78 to 93% (cVMS) and 76 to 102% (PCBs and benchmarks) in the  $K_{DOC}$  experiments ( $n = 4$ ) (see Table S4).

**Measurements.** The volatilization losses of the cVMS over time are shown in Figure 2 and those of the PCBs in Figure S1. In the similar studies conducted by Whelan et al.<sup>10,11</sup> for  $D_5$ , the fraction that was not available for volatilization was between 5% and 25%. When we treated the maximum amount of the nonavailable fraction,  $B$ , as an unconstrained fitting parameter, its value was unrealistically high in experiments where less than 60% of the spiked chemical was volatilized. We interpreted these high values of  $B$  as overfitting of the model and set a maximum limit for  $B$  of 20%. An exception was the case of  $D_4$ , where all volatilization from the system occurred in less than 24 h in each of the four replicate measurements of  $K_{OC}$  and  $K_{DOC}$ , and  $B$  was found to be between 16 and 35% (Tables S5 and S6).

The correlation coefficient ( $R^2$ ) for curve fits to the experimental data using eqs 4 and 5 ranged from 0.86 to 1 for the  $K_{OC}$  experiments and from 0.78 to 1 for the  $K_{DOC}$  experiments (Tables S5 and S6). The  $R^2$ s for  $D_5$  in both experiments are consistently lower than for the rest of the chemicals; the reason for that discrepancy is unknown. The  $MTC_a$  and  $MTC_w$  were nearly identical in the four replicates of the two experiments and averaged  $1.48 \pm 0.083$  m/h and  $0.0354 \pm 0.0038$  m/h, respectively.

We determined log  $K_{OC}$  of cVMS that ranged from 5.06 to 7.07 and log  $K_{OC}$  of the PCBs that ranged from 5.36 to 5.52 (Table 1). The measured log  $K_{DOC}$  of cVMS ranged from 5.05 to 6.79 and those of the PCBs from 5.36 to 6.04 (Table 1).

**PP-LFER Predictions Based on Literature Data.** PP-LFERs for  $K_{OC}$  trained with data from Nguyen et al.<sup>28</sup> and for Aldrich humic acid  $K_{DOC}$  from Neale et al.<sup>25</sup> (Table 2) predict our measured partition ratios for PCBs more accurately than for cVMS (Figure 3 A and B). The RMSEs for the cVMS are nearly 0.8 log units and the errors increase with increasing size of cVMS.

The  $K_{OC}$  PP-LFER trained with the data from Bronner et al.<sup>29</sup> (Table 2) showed larger errors in the predictions of both PCBs and cVMS compared to the Nguyen et al.<sup>28</sup> PP-LFER (Figure S2). Also in this case, the errors in the prediction for cVMS increase with increasing size of cVMS.

**Refining the Solvent Descriptors of the PP-LFERs.** Including our new measurements of  $K_{OC}$  for cVMS and PCBs in the training set of Nguyen et al.<sup>28</sup> and our measurements of

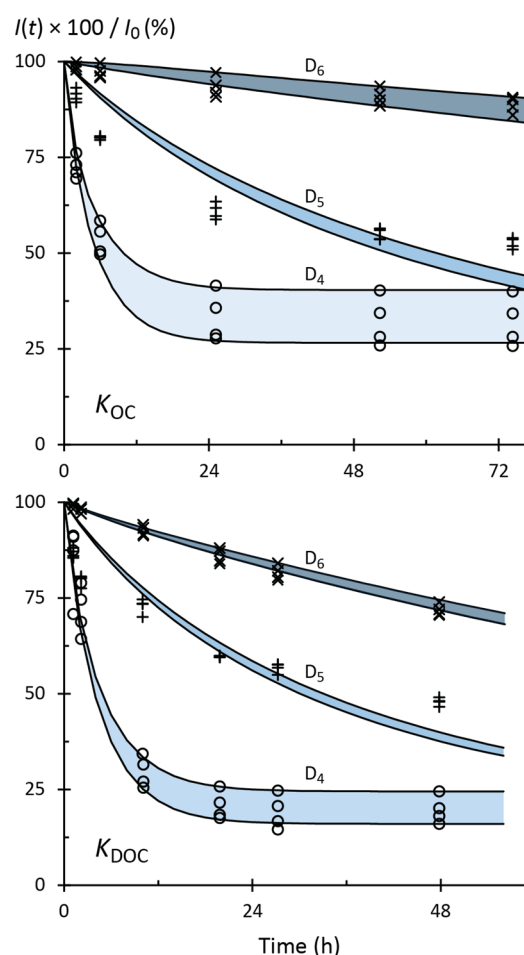


**Figure 2.** Percentage of spiked cVMS remaining in the experimental system as a function of time in four replicates of experiments to measure  $K_{OC}$  (top panel) and  $K_{DOC}$  (bottom panel). Symbols are experimental data for  $D_6$  (x),  $D_5$  (+), and  $D_4$  (O), and the lines and shaded areas show the range of the model fits using eqs 4 and 5.  $I(t)$  is the amount of the chemical that has not volatilized and been trapped by the ENV+ sorbent at time  $t$  and  $I_0$  is the amount spiked into the system.

**Table 1. Average Partition Ratios of cVMS and PCBs as Measured in This Study<sup>a</sup>**

	log $K_{OC}$	log $K_{DOC}$
D4	5.06 (0.08)	5.05 (0.07)
D5	6.12 (0.08)	6.13 (0.09)
D6	7.07 (0.10)	6.79 (0.04)
PCB 28	5.36 (0.35)	5.36 (0.48)
PCB 52	5.44 (0.10)	5.54 (0.27)
PCB 153	5.52 (0.21)	6.04 (0.08)

<sup>a</sup>The standard deviations of the 4 replicate measurements are shown in parentheses.

$K_{DOC}$  for cVMS and PCBs in the training set of Neale et al.<sup>25</sup> and recalculating the solvent descriptors (Table 2) improved the fit to the measurements for both PP-LFERs (Figure 3, C and D). The largest errors occurred in the predictions of log  $K_{DOC}$ , but RMSEs for the new PP-LFERs are in all cases less than 0.5 log units (Figure 3 C and D). Including our new measurements of  $K_{OC}$  for cVMS and PCBs in the training set of Bronner et al.<sup>29</sup> and recalculating the solvent descriptors (Figure S2) also improved the fit to our measurements of  $K_{OC}$

Table 2. Solvent Descriptors for the  $\log K_{OC}$  and the  $\log K_{DOC}$  PP-LFERs<sup>a</sup>

When Our Measurements for $K_{OC}$ and $K_{DOC}$ of cVMS and PCBs Are Not Included in the Training Set of the PP-LFERs						
	<i>s</i>	<i>a</i>	<i>b</i>	<i>v</i>	<i>l</i>	<i>c</i>
$\log K_{OC}$ Nguyen data set <sup>28</sup>	−0.62	−0.48	−2.26	1.44	0.44	−0.03
$\log K_{OC}$ Bronner data set <sup>29</sup>	−0.99	−0.42	−3.34	1.21	0.54	0.01
$\log K_{DOC}$ Neale data set <sup>25</sup>	−0.76	0.3	−3.19	2.27	0.45	−0.74
When Our Measurements for $K_{OC}$ and $K_{DOC}$ of cVMS and PCBs Are Included in the Training Set of the PP-LFERs						
	<i>s</i>	<i>a</i>	<i>b</i>	<i>v</i>	<i>l</i>	<i>c</i>
$\log K_{OC}$ Nguyen data set <sup>28</sup>	−0.68	−0.45	−2.14	1.74	0.40	−0.11
$\log K_{OC}$ Bronner data set <sup>29</sup>	−0.76	−0.25	−3.73	2.04	0.39	−0.32
$\log K_{DOC}$ Neale data set <sup>25</sup>	−0.80	0.19	−3.02	1.84	0.52	−0.55

<sup>a</sup>The two datasets that were used as training sets for  $\log K_{OC}$  were compiled by Nguyen et al.<sup>28</sup> and Bronner et al.<sup>29</sup>, and the data set that was used as training set for  $\log K_{DOC}$  was compiled by Neale et al.<sup>25</sup>.

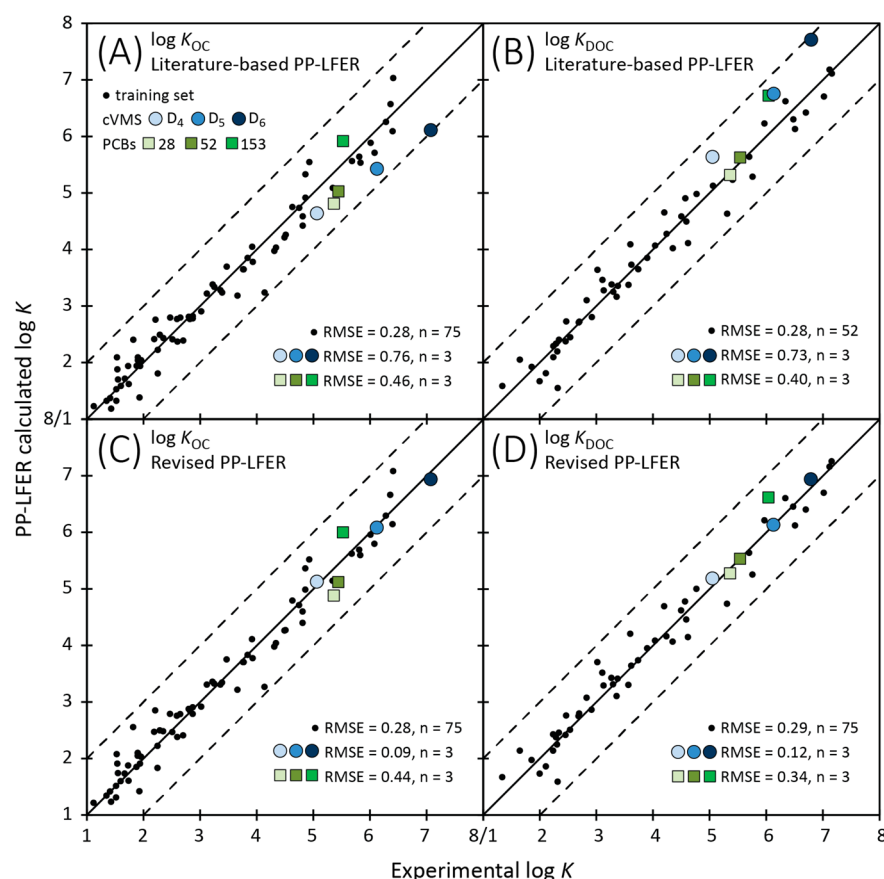


**Figure 3.** Literature PP-LFER-derived  $\log K_{OC}$  and  $\log K_{DOC}$  (A and B) versus revised PP-LFER predictions of  $\log K_{OC}$  and  $\log K_{DOC}$  (C and D) with our measurements included in the training set of the PP-LFERs. Literature-based PP-LFER for  $\log K_{OC}$  refers to the PP-LFER constructed based on the data set compiled by Nguyen et al.<sup>28</sup> and literature-based PP-LFER for  $\log K_{DOC}$  refers to the PP-LFER constructed using the data set compiled by Neale et al.<sup>29</sup> Revised PP-LFERs refer to the PP-LFERs constructed using the previously mentioned data sets including our measurements. Solid lines show 1:1 agreement and dashed lines show  $\pm 1$  log unit deviation from the 1:1 line.

for cVMS and PCBs by decreasing the RMSE of cVMS from 3.55 to 0.19 and the RMES of the PCBs from 0.84 to 0.25. However, in this case the RMSE for the training set increased by 0.21 log units from 0.46 to 0.67.

## DISCUSSION

**Measurements.** Total recoveries of the chemicals ranged from 70 to 108%, indicating that some losses occurred during most of the experiments. Possible loss mechanisms include formation of a nonavailable fraction that resisted our solvent extraction, hydrolysis, leakage when changing cartridges, and

breakthrough. The PCBs are not expected to be degraded in the experiments, thus the lack of a closed mass balance may indicate that there are two types of nonavailable fractions in the system; one fraction that is not available for extraction with water and subsequent volatilization and one that is not available for extraction with organic solvents. This may also apply to cVMS, although the case of cVMS is more complex because of the possibility of hydrolysis. Hydrolysis of cVMS depends on pH and temperature.<sup>1–3</sup> Although the pH of the water was adjusted to neutral before each experiment, there might have been a fraction of cVMS that was subjected to hydrolysis during

the experiment. Nonetheless, the lost fraction is for all cases at maximum 30% of the spiked amount of chemical in the system.

Our measured partition ratios of the PCBs are in good agreement with previous measurements<sup>30,31</sup> and with the estimates given by PP-LFERs derived from literature data (Figure 3, parts A and B), with the exception of  $K_{\text{DOC}}$  for PCB153 for which our measured value is 0.8 log units higher than predicted by the PP-LFER. Our measured values of log  $K_{\text{OC}}$  and log  $K_{\text{DOC}}$  of  $D_5$  are in good agreement with the measurements of Whelan et al.<sup>10,11</sup> and 0.93 log units higher than the measurements of Kozerski et al.<sup>16</sup> Our measured log  $K_{\text{OC}}$  of  $D_4$  is similarly 0.83 log units higher than the measurements of Kozerski et al.<sup>16</sup> The differences observed between our measurements and those of Whelan et al.<sup>10,11</sup> and Kozerski et al.<sup>16</sup> (Table S8) could be attributed to a myriad of factors, including differences in the source of organic carbon, differences in dosing the chemicals on the organic carbon and differences in the experimental setup. Whelan et al.<sup>11</sup> used suspended particles in river water as a source of organic carbon, Kozerski et al.<sup>16</sup> used soil and in our study we used sediment. Since organic carbon is not a well-defined standard material such as for example octanol, differences in the molecular composition of the source of organic carbon may result in differences in the partitioning of a chemical between organic carbon and water. In the study of Whelan et al.,<sup>11</sup> water containing suspended particles was spiked with  $D_5$ , and the  $K_{\text{OC}}$  was calculated based on the volatilization rate of the chemicals from the system. In the study of Kozerski et al.,<sup>16</sup>  $D_4$  and  $D_5$  were spiked to a soil/water slurry and the system was let to equilibrate. After equilibration, the two phases were extracted separately, and the  $K_{\text{OC}}$  was calculated based on the determined concentrations. These differences in the experimental setup can perhaps explain the differences in the measured  $K_{\text{OC}}$ . However, the exact mechanism behind those differences remains unknown.

The good agreement of our measurements for the PCBs with the estimates given by the PP-LFERs and good agreement between our measurements for  $D_4$  and  $D_5$  with other reports<sup>10,11,16</sup> leads us to the conclusion that the assumptions we made about formation of the nonavailable fraction and equilibrium in the water phase were reasonable.

The main reason that we preferred our measurements of the log  $K_{\text{OC}}$  and log  $K_{\text{DOC}}$  of cVMS to train the PP-LFERs is that our study is the only study that presents measurements for  $D_4$ ,  $D_5$ , and  $D_6$ , where all measurements were made with the same method. Another reason is that our study is the only study that uses reference chemicals (PCBs) that provide confidence the method is working as intended, which provides an extra degree of confidence to our results.

The measured log  $K_{\text{OC}}$  values in the data sets of Nguyen et al.<sup>28</sup> and Neale et al.<sup>25</sup> span from 1.12 to 6.41 and from 1.34 to 7.16, respectively, covering the range of our measured log  $K_{\text{OC}}$  values for the reference chemicals and for most of cVMS. The data set of Bronner et al.<sup>29</sup> has a smaller range of log  $K_{\text{OC}}$  spanning from 0.64 to 4.39. All our measurements are higher than 4.39 and therefore they could be considered outside the application domain of the Bronner et al.<sup>29</sup> PP-LFER. However, the chemical applicability domain is not related only to the range of  $K_{\text{OC}}$  measurements but also to the underlying molecular descriptors of the substances used in the training set of the PP-LFER. The Bronner et al.<sup>29</sup> data set set had the largest range in polar descriptors (A,B,S), while the Nguyen et al.<sup>28</sup> data set had a wider range in the apolar descriptors

(L,V,E). cVMS have exceptionally low  $L$  values compared to their  $V$ . Therefore, the training set of Nguyen might be more appropriate in this case. In any other case where we would deal with a data set of highly diverse compounds we would recommend using the Bronner et al. data set.<sup>29</sup>

Our  $K_{\text{OC}}$  measurements for cVMS are 1.22–1.53 log units lower than the  $K_{\text{OC}}$  estimates given by the Seth regression and about 0.8 log units higher than the estimates given by a PP-LFER trained with  $K_{\text{OC}}$  measurements from the literature (Figure 3 A). Thus, neither the Seth regression nor a PP-LFER trained with literature data for non-cVMS chemicals provided a satisfactory estimate of our measured  $K_{\text{OC}}$ .

In the  $K_{\text{DOC}}$  experiments, we measured sorption to the fraction of Aldrich humic acid that passed a glass fiber filter with a pore size of 1.2  $\mu\text{m}$  to replicate Whelan et al.'s experimental method.<sup>10,11</sup> The training data set from Neale et al.<sup>25</sup> for  $K_{\text{DOC}}$  is from studies that used Aldrich humic acid sodium salt as a source of DOC. This difference could have resulted in underestimation or overestimation of the  $K_{\text{DOC}}$  measurements because of potential differences in the size of the dissolved matter or because of a salting-out effect from dissolved salts. However, our measured  $K_{\text{DOC}}$  for two of the three PCBs and for  $D_5$  were consistent with those reported in the literature<sup>31,10</sup> and also in good agreement with the PP-LFER estimates when our measurements were included in the training set (Figure 3D).

PP-LFERs can in principle be applied to describe the partitioning of diverse chemicals, but none of the PP-LFERs that were tested in this study performed well when cVMS were not included in the training set, indicating that cVMS were outside the domain of applicability of the PP-LFERs. cVMS have a lower hexadecane/air partition ratio ( $L$ ) than nonsilicon containing compounds with similar McGowan's molecular volume ( $V$ ).<sup>22</sup>  $L$  is governed by London dispersive forces and dipole–induced dipole interactions, and therefore low  $L$  signifies low tendency for London dispersive forces and dipole–induced dipole interactions. Silicon has a higher  $V$  than carbon and has a larger and more loosely held electron cloud.<sup>32,33</sup> However, in cVMS, the Si atoms are all located in a ring and bonded to two methyl groups that may hinder their participation in London interactions with other molecules. The silicon is less electronegative than carbon, so in principle one would expect stronger dipoles in Si–O bonds compared to C–O bonds. However, the Si–O bonds in cVMS are arranged in a symmetrical ring structure of alternating (–O–Si–O–) and therefore two O atoms pull the Si electrons in opposite directions.<sup>32</sup> This simultaneous attraction weakens the permanent dipoles between O and Si.<sup>32</sup> In addition, the structure of the ring may hinder the accessibility of the permanent dipoles and may not be able to induce dipoles in hexadecane. Evidence of the steric hindrance of the ring structure of cVMS reducing the potential for London forces and dipole–induced dipole interactions can be found in comparing the log  $K_{\text{OC}}$  of the cyclic  $D_4$  to linear decamethyltetrasiloxane ( $L_4$ ). Kozerski<sup>16</sup> found log  $K_{\text{OC}}$  values of 4.22 for  $D_4$  and 5.16 for  $L_4$ .

**Differences in Sorption between OC and DOC.** As discussed above, cVMS have a lower  $L$  compared to other chemicals with similar  $V$ . For that reason, we focused the comparison of OC and DOC on their differences in  $v$  and  $l$ . In the PP-LFER equations that include cVMS in the training set  $v_{\text{DOC}}$  is slightly larger than  $v_{\text{OC}}$  (1.84 and 1.76) (Figure 3) implying that the energy cost for cavity formation on the water

side will be slightly higher in a  $K_{\text{DOC}}$  system than in a  $K_{\text{OC}}$  system. Water is a highly cohesive solvent, and the high energy cost for cavity formation in water is evident in the positive sign in both descriptors, which implies that larger  $V$  molecules have larger  $K_{\text{OC}}$  and  $K_{\text{DOC}}$ . This positive contribution is shown in Figure 4, where the  $\nu V$  for both  $K_{\text{DOC}}$  and  $K_{\text{OC}}$  has a positive sign.

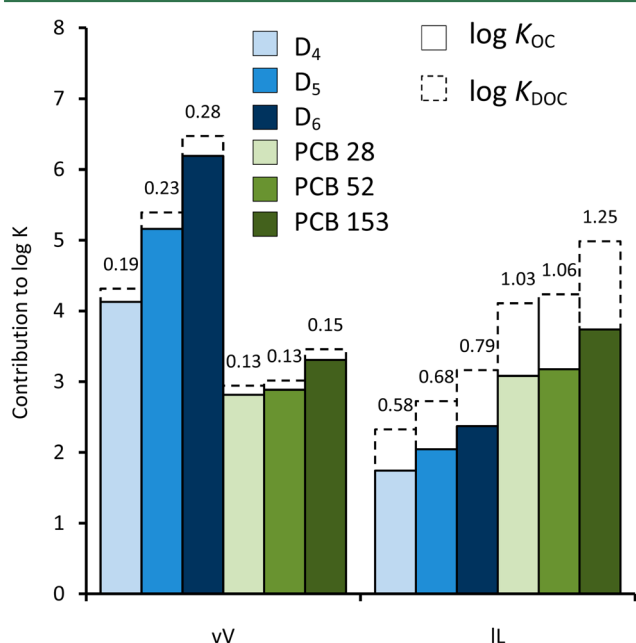


**Figure 4.** Contributions of the solute and solvent descriptors to  $\log K_{\text{OC}}$  and  $\log K_{\text{DOC}}$  according to the new PP-LFERs of the VL model. The solid columns show the contributions of  $\nu V$  and  $IL$  to  $\log K_{\text{OC}}$ , while the empty columns show the contributions of  $\nu V$  and  $IL$  to  $\log K_{\text{DOC}}$ . The numbers above the columns show the differences between the contributors of  $K_{\text{DOC}}$  and  $K_{\text{OC}}$  for each chemical ( $\nu V_{\text{DOC}} - \nu V_{\text{OC}}$  and  $IL_{\text{DOC}} - IL_{\text{OC}}$ ).

For the PP-LFER equations that include cVMS in the training set (Table 2)  $l_{\text{DOC}}$  exceeds  $l_{\text{OC}}$  (0.52 versus 0.39). The positive sign of  $l_{\text{DOC}}$  and  $l_{\text{OC}}$  indicates that DOC and OC participate in London dispersive forces and dipole-induced dipole interactions more effectively than water, which implies that higher  $L$  molecules have higher  $K_{\text{DOC}}$  and  $K_{\text{OC}}$ . DOC participates more effectively in London dispersive forces and dipole-induced dipole interactions than OC. Water molecules have permanent dipoles ( $\delta^+$  and  $\delta^-$ ) that can induce dipoles to a solute forming dipole-induced dipole interactions. However, since both DOC and OC offer more available sites for London dispersive forces and dipole-induced dipole interactions than water, the difference in the tendencies of the two phases will be positive and will have a positive contribution to  $K_{\text{DOC}}$  and  $K_{\text{OC}}$ . This positive contribution is shown in Figure 4 where the  $IL$  for both  $K_{\text{DOC}}$  and  $K_{\text{OC}}$  has a positive sign.

**Differences in Sorption between cVMS and PCBs.** Figure 4 shows larger differences between  $\nu V_{\text{OC}}$  and  $\nu V_{\text{DOC}}$  for cVMS (0.19, 0.23, 0.28) than for PCBs (0.13, 0.13, 0.15). Changes in the matrix that affect  $\nu$  have a stronger effect on cVMS than on PCBs. Figure 4 also shows smaller differences between  $IL_{\text{OC}}$  and  $IL_{\text{DOC}}$  for cVMS (0.58–0.79) than for PCBs (1.03–1.25), hence, changes in the matrix that affect  $l$  have a weaker effect on cVMS than on PCBs.

**Implications for Partitioning of cVMS.** It is notable that SP-LFERs trained with substances other than cVMS overestimated the  $\log K_{\text{OC}}$  and  $\log K_{\text{DOC}}$  of cVMS that we measured, and PP-LFERs that do not include cVMS in their training set underestimated the  $\log K_{\text{OC}}$  and  $\log K_{\text{DOC}}$ . Thus, when using multimedia models to describe the fate of cVMS in the environment care must be taken to ensure partitioning to organic carbon is not incorrectly described by default model algorithms.

Our results corroborate the findings of Endo and Goss<sup>22</sup> who demonstrated that the composition of the training set of a PP-LFER plays an important role in the accurate description of the partition ratios of cVMS. Our new PP-LFERs that include cVMS in the training set describe our measurements with an error of less than half an order of magnitude. However, it remains unclear whether these equations can predict partition ratios for other siloxane chemicals not included in the training set. The  $K_{\text{OC}}$  and  $K_{\text{DOC}}$  PP-LFERs we derived here should be further evaluated and possibly recalibrated when good quality experimental measurements for other siloxanes become available. Furthermore, it is also recommended to compare these data across different types of OC (e.g., soil, sediment, impacted sediment, sewage sludge), to check for variations in sorption caused by variations in the molecular composition of the OC source.

## ■ ASSOCIATED CONTENT

### Supporting Information

The Supporting Information is available free of charge on the ACS Publications website at DOI: 10.1021/acs.est.5b02483.

Description of the experimental conditions and procedures, Figures and Tables (PDF)

## ■ AUTHOR INFORMATION

### Corresponding Author

\*Phone: +4686747565; e-mail: dimitrios.panagopoulos@aces.su.se (D.P.).

### Notes

The authors declare no competing financial interest.

## ■ ACKNOWLEDGMENTS

This study was funded by the Swedish Research Council FORMAS (2011-484). We thank Suzana Stojanovic for her assistance with the experimental work. We kindly acknowledge the three anonymous reviewers whose insightful comments helped to improve the manuscript.

## ■ REFERENCES

- (1) Brooke, D. N.; Crookes, M. J.; Gray, D.; Robertson, S. Risk Assessment Report: Octamethylcyclotetrasiloxane. *Environment Agency of Great Britain*, 2009.
- (2) Brooke, D. N.; Crookes, M. J.; Gray, D.; Robertson, S. Risk Assessment Report: Decamethylcyclopentasiloxane. *Environment Agency of Great Britain*, 2009.
- (3) Brooke, D. N.; Crookes, M. J.; Gray, D.; Robertson, S. Risk Assessment Report: Dodecamethylcyclohexasiloxane. *Environment Agency of Great Britain*, 2009.
- (4) Sparham, C.; van Egmond, R.; Hastie, C.; O'Connor, S.; Gore, D.; Chowdhury, N. Determination of decamethylcyclopentasiloxane in river and estuarine sediments in the UK. *J. Chromatogr. A* **2011**, *1218* (6), 817–823.
- (5) Borgå, K.; Fjeld, E.; Kierkegaard, A.; McLachlan, M. S. Consistency in trophic magnification factors of cyclic methyl siloxanes



in pelagic freshwater food webs leading to brown trout. *Environ. Sci. Technol.* **2013**, *47*, 14394–14402.

(6) Xu, S.; Kropscott, B. Method for simultaneous determination of partition coefficients for cyclic volatile methylsiloxanes and dimethylsilanediol. *Anal. Chem.* **2012**, *84*, 1948–1955.

(7) Atkinson, R. Kinetics of the gas phase reactions of a series of organosilicon compounds with OH and NO<sub>3</sub> radicals and O<sub>3</sub> at 297 ± 2 K. *Environ. Sci. Technol.* **1991**, *25* (5), 863–866.

(8) McLachlan, M.; Kierkegaard, A.; Hansen, K. M.; van Egmond, R.; Christensen, J. H.; Skjøth, C. A. Concentrations and fate of decamethylcyclopentasiloxane (D<sub>5</sub>) in the atmosphere. *Environ. Sci. Technol.* **2010**, *44*, 5365–5370.

(9) Safron, A.; Strandell, M.; Kierkegaard, A.; MacLeod, M. Rate constants and activation energies for gas-phase reactions of three cyclic volatile methyl siloxanes with the hydroxyl radical. *Int. J. Chem. Kinet.* **2015**, *47*, 420–428.

(10) Whelan, M. J.; Sanders, D.; van Egmond, R. Effect of Aldrich humic acid on water-atmosphere transfer of decamethylcyclopentasiloxane. *Chemosphere* **2009**, *74* (8), 1111–1116.

(11) Whelan, M. J.; van Egmond, R.; Gore, D.; Sanders, D. Dynamic multi-phase partitioning of decamethylcyclopentasiloxane (D<sub>5</sub>) in river water. *Water Res.* **2010**, *44* (12), 3679–3686.

(12) Seth, R.; Mackay, D.; Muncke, J. Estimating the organic carbon partition coefficient and its variability for hydrophobic chemicals. *Environ. Sci. Technol.* **1999**, *33* (14), 2390–2394.

(13) Karickhoff, S. W.; Brown, D. S.; Scott, T. A. Sorption of hydrophobic pollutants on natural sediments. *Water Res.* **1979**, *13*, 241–248.

(14) Karickhoff, S. W. Semi-empirical estimation of sorption of hydrophobic pollutants on natural sediments and soils. *Chemosphere* **1981**, *10* (8), 833–846.

(15) Burkhard, L. P. Estimating dissolved organic carbon partition coefficients for nonionic organic chemicals. *Environ. Sci. Technol.* **2000**, *34* (22), 4663–4668.

(16) Kozerski, G. E.; Xu, S.; Miller, J.; Durham, J. Determination of soil-water partition coefficients of volatile methylsiloxanes. *Environ. Toxicol. Chem.* **2014**, *33* (9), 1937–1945.

(17) Schwarzenbach, R. P.; Gschwend, P. M.; Imboden, D. M. *Environmental Organic Chemistry*; John Wiley & Sons Inc.: New York, 2003.

(18) Endo, S.; Goss, K.-U. Applications of polyparameter linear free energy relationships in environmental chemistry. *Environ. Sci. Technol.* **2014**, *48*, 12477–12491.

(19) Abraham, M. H. Scales of solute hydrogen-bonding: Their construction and application to physicochemical and biochemical processes. *Chem. Soc. Rev.* **1993**, *22* (2), 73–83.

(20) Abraham, M. H.; Ibrahim, A.; Zissimos, A. M. Determination of sets of solute descriptors from chromatographic measurements. *J. Chromatogr. A* **2004**, *1037*, 29–47.

(21) Goss, K.-U. Predicting the equilibrium partitioning of organic compounds using just one linear solvation energy relationship (LSER). *Fluid Phase Equilib.* **2005**, *233* (1), 19–22.

(22) Endo, S.; Goss, K.-U. Predicting partition coefficients of polyfluorinated and organosilicon compounds using polyparameter linear free energy relationships (PP-LFERs). *Environ. Sci. Technol.* **2014**, *48*, 2776–2784.

(23) Kierkegaard, A.; McLachlan, M. Determination of decamethylcyclopentasiloxane in air using commercial solid phase extraction cartridges. *J. Chromatogr. A* **2010**, *1217*, 3557–3560.

(24) Niederer, C.; Goss, K.-U.; Schwarzenbach, R. P. Sorption equilibrium of a wide spectrum of organic vapors in Leonardite humic acid: modeling of experimental data. *Environ. Sci. Technol.* **2006**, *40*, 5374–5379.

(25) Neale, P. A.; Escher, B. I.; Goss, K.-U.; Endo, S. Evaluating dissolved organic carbon-water partitioning using polyparameter linear free energy relationships: Implications for the fate of disinfection by-products. *Water Res.* **2012**, *46*, 3637–3645.

(26) Jahnke, A.; Mayer, P.; McLachlan, M. S.; Wickström, H.; Gilbert, D.; MacLeod, M. Silicone passive equilibrium samplers as

'chemometers' in eels and sediments of a Swedish lake. *Environ. Sci.: Processes Impacts* **2014**, *16*, 464–472.

(27) Harris, D. C. Nonlinear least-squares curve fitting with Microsoft Excel Solver. *J. Chem. Educ.* **1998**, *75* (1), 119–121.

(28) Nguyen, T. H.; Goss, K.-U.; Ball, W. P. Polyparameter linear free energy relationships for estimating the equilibrium partition of organic compounds between water and the natural organic matter in soils and sediments. *Environ. Sci. Technol.* **2005**, *39* (4), 913–924.

(29) Bronner, G.; Goss, K.-U. Predicting sorption of pesticides and other multifunctional organic chemicals to soil organic carbon. *Environ. Sci. Technol.* **2011**, *45*, 1313–1319.

(30) Cortes, A.; Riego, J.; Paya-Perez, A. B.; Larsen, B. Soil sorption of co-planar and non-planar PCBs. *Toxicol. Environ. Chem.* **1991**, *31*, 79–86.

(31) Durjava, M. K.; ter Laak, T. L.; Hermens, J. L. M.; Struijs, J. Distribution of PAHs and PCBs to dissolved organic matter: High distribution coefficients with consequences for environmental fate modeling. *Chemosphere* **2007**, *67*, 990–997.

(32) Housecroft, C.; Sharpe, A. G. *Inorganic Chemistry*; Pearson Education Inc.: New York, 2012.

(33) McGowan, J. C. Molecular volumes and structural chemistry. *Recueil des Travaux Chimiques des Pays-Bas* **1956**, *75*, 193–208.